Biochemical and Biophysical Research Communications 451 (2014) 442–448

Contents lists available at ScienceDirect

Biochemical and Biophysical Research Communications

journal homepage: www.elsevier.com/locate/ybbrc

Skeletal analysis and differential gene expression in Runx2/Osterix double heterozygous embryos

Ji-Eun Baek [a,b], Je-Yong Choi [a,c,d], Jung-Eun Kim [a,b,d,*]

[a] Cell and Matrix Research Institute, Kyungpook National University School of Medicine, Daegu 700-422, Republic of Korea
[b] Department of Molecular Medicine, Kyungpook National University School of Medicine, Daegu 700-422, Republic of Korea
[c] Department of Biochemistry and Cell Biology, Kyungpook National University School of Medicine, Daegu 700-422, Republic of Korea
[d] BK21 Plus KNU Biomedical Convergence Program, Department of Biomedical Science, Kyungpook National University, Daegu 700-422, Republic of Korea

ARTICLE INFO

Article history:
Received 20 July 2014
Available online 9 August 2014

Keywords:
Runx2
Osterix
Double heterozygotes
Bone
DNA microarray

ABSTRACT

The transcription factors, Runx2 and Osterix (Osx), act downstream in the BMP2 pathway, and they are essential for osteoblast differentiation and bone formation. While Runx2 expression is normal in Osx-null mice, Osx is not expressed in Runx2-null mice, indicating that Osx acts downstream of Runx2 during bone formation. Runx2 and Osx are also independently regulated during bone formation. To define the unknown correlation between Runx2 and Osx in the regulation of bone formation, we analyzed the bone of Runx2/Osx double heterozygotes generated by mating heterozygous Runx2 and Osx mice and elucidated the differential gene expressions due to the lack of Runx2 and Osx in bone. Compared to the Runx2 and Osx heterozygous embryos, Runx2/Osx double heterozygous embryos showed reduced bone length in the humerus and femur as well as hypoplastic or complete absence of the maxillary and palatine shelf, presphenoid bone, zygomatic bone, and tympanic ring. Severe inward bending was observed in the ribs and humerus. Histological analysis showed an expanded region of hypertrophic chondrocytes and a reduced area of mineralized bones in the Runx2/Osx double heterozygous embryos. DNA microarray analysis of the calvaria of embryos allowed gene classification based on similarities in the upregulated and downregulated expression patterns. Clusters 1 and 2 include 68 downregulated genes and 18 upregulated genes, respectively, in the Runx2/Osx double heterozygous embryos. Finally, the skeletal analysis and gene expression profiles obtained by clustering may facilitate the understanding of the correlation between Runx2 and Osx in skeletal development.

1. Introduction

The bone morphogenetic protein (BMP) signaling pathway is essential for osteogenesis in bone. Previous *in vitro* and *in vivo* studies have been reported the importance of BMP signaling in bone formation. Osteoblast-specific Bmpr1a-deficient mice show a reduced rate of bone formation due to impaired osteoblast function and increased bone volume due to reduced osteoclastic bone resorption [1]. The osteoblast-specific overexpression of noggin, a BMP inhibitor, reduces bone mineral density and the rate of bone formation [2,3]. Mice with a targeted disruption of Tob, which is a member of a new antiproliferative protein family and represses BMP-induced Smad-dependent transcription in osteoblasts, show increased bone mass and accelerated bone formation [4]. BMP signaling is also known to control the expression and function of Runx2 through Smad signaling [5,6]. These results indicate that BMPs are key molecules that regulate bone formation and remodeling.

Runt-related transcription factor 2 (Runx2) and Osterix (Osx) are master transcription factors that are downstream genes of BMP during osteogenesis. Runx2 is expressed in all chondrocytes and osteoblasts, and it plays multiple roles in the processes of chondrogenesis and osteogenesis. Runx2-deficient ($Runx2^{-/-}$) or C-terminus truncated Runx2 ($Runx2^{\Delta C/\Delta C}$) mice exhibit a complete lack of both intramembranous and endochondral ossification due to the absence of osteoblast differentiation. However, Runx2 heterozygous mice ($Runx2^{+/-}$ or $Runx2^{\Delta C/+}$) have a normal phenotype, except for missing clavicles and cranial abnormality [7–9]. Osx is specifically expressed in the bones and is crucial for osteoblast differentiation and bone formation. Osx-deficient mice ($Osx^{-/-}$) show a complete lack of osteoblast differentiation coupled with the absence of bone formation, whereas Osx heterozygous mice ($Osx^{+/-}$) are fertile with a normal skeleton [10]. Remarkably, Runx2

* Corresponding author at: Department of Molecular Medicine, Cell and Matrix Research Institute, Kyungpook National University School of Medicine, 101 Dongin-dong, Jung-gu, Daegu 700-422, Republic of Korea. Fax: +82 53 426 4944.
E-mail address: kjeun@knu.ac.kr (J.-E. Kim).

http://dx.doi.org/10.1016/j.bbrc.2014.08.010
0006-291X/

is normally expressed in the mesenchymal cells of Osx-null mutants, while the expression of Osx is absent in Runx2-null mutants. This indicates that Osx acts downstream of Runx2 during osteogenesis [10].

Recently, BMP signaling was found to be necessary for the Runx2-dependent induction of osteogenic gene expression in osteoblast differentiation [11]. However, BMP2 was also found to induce Osx independent of the Runx2 pathway *in vitro*. While Runx2 expression was induced by BMP2 and mediated by Dlx5 [12], Osx expression was mainly induced by BMP2, but not by blocking Dlx5 in Runx2-null cells [13]. Thus, Dlx5 is a general mediator that regulates the expression of Runx2 and Osx via an independent pathway. In addition, Osx is regulated via both Runx2-dependent and Runx2-independent pathways, and it controls osteoblast differentiation by regulating the expression of genes that are not controlled by Runx2 [14]. These results indicate that Osx expressed in the bone may not be entirely regulated by Runx2. However, it has not been well studied about the correlation between Runx2 and Osx, as well as the BMP-Runx2-Osx pathway. To find the correlation between Runx2 and Osx in bone formation, here, we investigated skeletal alterations and differential gene expression in Runx2 and Osx double deficiency. Runx2 and Osx double heterozygotes were generated by intercrossing C-terminus truncated Runx2 male mice ($Runx2^{\Delta C/+}$) and heterozygous Osx female mice ($Osx^{+/-}$). These embryos showed decreased bone length, abnormal phenotypes, and delayed bone formation compared to the other embryos. DNA microarray was performed using the calvaria of the embryos to profile the expression of genes altered by Runx2 and Osx deficiency. Eventually, the histological analysis and gene expression profiles in response to the lack of both Runx2 and Osx should be useful for demonstrating the correlation between Runx2 and Osx in bone formation.

2. Materials and methods

2.1. Mouse generation

Runx2 C-terminus truncated mice ($Runx2^{\Delta C/+}$) [7] were crossed with Osx heterozygous mice ($Osx^{+/-}$) [10] to generate $Runx2^{+/+}$;$Osx^{+/+}$ (wild-type, WT), $Runx2^{\Delta C/+}$;$Osx^{+/+}$ ($Runx2^{het}$), $Runx2^{+/+}$;$Osx^{+/-}$ (Osx^{het}), and $Runx2^{\Delta C/+}$;$Osx^{+/-}$ double heterozygotes ($Double^{het}$). PCR genotyping for Runx2 and Osx was performed on genomic DNA isolated from the embryo tail using the HiYield Genomic DNA mini kit (RBC, Taiwan). All procedures concerning animal experiments were conducted with the approval of Kyungpook National University.

2.2. Skeletal preparation

Mouse skeletons at 17.5 days post coitum (dpc) were prepared and treated with alcian blue to stain the cartilage and alizarin red S to stain the bone. Briefly, the skin and viscera were removed, and mice were fixed in 95% ethanol overnight and stained overnight in 150 mg/l alcian blue solution (Sigma–Aldrich, St. Louis, MO, USA) with 20% acetic acid and 80% ethanol. The carcasses were rinsed in 95% ethanol for at least 3 h and treated in 2% KOH for 24 h to clarify the soft tissues. The bones were then stained in 50 mg/l alizarin red S (Sigma–Aldrich, St. Louis, MO, USA) in 1% KOH. Finally, the skeletons were cleared in 1% KOH/20% glycerol for at least 2 days.

2.3. Histological analyses

For histological analysis, mice were sacrificed at 15.5 and 17.5 dpc. Embryos were fixed in 4% paraformaldehyde at 4 °C overnight and dehydrated in an ethanol series. The samples were embedded in paraffin and cut into 5 μm sections. For hematoxylin and eosin (H&E) staining, the sections were deparaffinized in Histoclear II (National Diagnostics, Atlanta, GA, USA) and rehydrated in a graded series of ethanol. After incubation with hematoxylin (Zymed, San Francisco, CA, USA) for 1 min, the sections were washed and stained with 0.25% eosin Y (Sigma–Aldrich, St. Louis, MO, USA) for 10 s. For alcian blue staining, deparaffinized sections were incubated with 0.1 N HCl for 5 min. The sections were then stained with alcian blue in 0.1 N HCl for 5 min, rinsed in 0.1 N HCl for 5 min, and counterstained with nuclear fast red. For the von Kossa staining, the deparaffinized slides were incubated with 1% silver nitrate solution placed under UV light for 5 min, and reacted with 5% sodium thiosulfate for 5 min.

2.4. RNA isolation and microarray

Total RNA was isolated from the calvaria at 17.5 dpc using TRI REAGENT™ (Sigma–Aldrich, St. Louis, MO, USA). Briefly, the tissue samples were homogenized in TRI REAGENT and placed at room temperature for 5 min. The upper aqueous phase from the sample mixture was collected by centrifugation, and mixed with 0.5 ml isopropanol to precipitate the RNA. The RNA pellet was washed in 75% ethanol, air-dried, and dissolved in water. Total RNA with a high RNA integrity number and a 260/280 absorbance ratio ranging from 1.8 to 2.1 was used for cDNA synthesis. cDNA synthesis was performed using the SuperScript® III First-Strand Synthesis System (Invitrogen, Carlsbad, CA, USA). The data for gene expression profiling were analyzed using GeneChip® Mouse Gene 1.0 ST

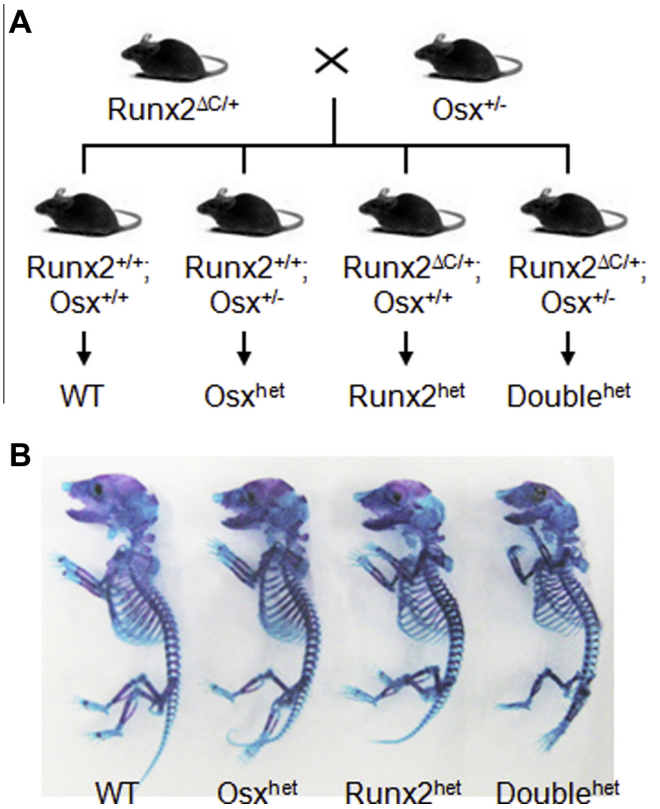

Fig. 1. Generation of Runx2/Osx double heterozygote ($Double^{het}$) embryos. (A) Breeding scheme to generate $Double^{het}$ embryos. Runx2 C-terminus truncated heterozygotes ($Runx2^{\Delta C/+}$) were crossed with $Osx^{+/-}$ heterozygotes to obtain WT, $Runx2^{het}$, Osx^{het}, and $Double^{het}$ animals. (B) Skeletal phenotypes in 17.5 dpc embryos. Skeletons were stained with alcian blue and alizarin red for cartilage and bone, respectively. $Double^{het}$ embryos were small and fragile compared to other embryos. (For interpretation of the references to color in this figure legend, the reader is referred to the web version of this article.)

array (Affymetrix, Santa Clara, CA, USA) containing 28,853 gene-level probe sets.

2.5. Statistical analysis

Statistical analysis was assessed by one way analysis of variance (ANOVA), and p values less than 0.05 ($p < 0.05$) were considered to be statistically significant.

3. Results

3.1. Abnormal phenotype and reduced bone growth in Double^{het} embryos

To investigate the Double^{het} bone phenotype, embryos were obtained by intercrossing Runx2 and Osx heterozygous mice (Fig. 1A). At 17.5 dpc, skeletons were prepared from the embryos and treated with alcian blue to stain cartilages and alizarin red S to stain the bones. Double^{het} embryos were smaller than their counterparts at 17.5 dpc (Fig. 1B). The skull bones were hypoplastic or entirely missing in the Double^{het} embryos. In particular, cranioskeletal hypoplasia or complete absence was evident in the maxillary and palatine shelf, presphenoid bone, zygomatic bone, and tympanic ring (Fig. 2A). Notably, severe inward bendings were observed in the ribs and humerus of Double^{het} embryos. Pelvic girdles and deltoid tuberosities were also hypoplastic or absent, and rib cages were small and fragile. Compared to Runx2^{het} and Osx^{het} embryos, Double^{het} embryos showed a significant decrease in the length of the long bones including the humerus and femur (Fig. 2B).

3.2. Delayed bone formation in Double^{het} embryos

Double^{het} embryos appeared phenotypically abnormal, having reduced bone length and impaired bone formation. When histological analysis was performed on the humerus of each embryo at 14.5, 15.5, 17.5, and 18.5 dpc, no difference in phenotype was observed between Double^{het} embryos and the other embryos at 14.5 dpc (data not shown). At 15.5 dpc, normal bone formation was observed in the WT embryos (Fig. 3). The pattern of bone formation was very similar in the WT and Osx^{het} embryos (data not shown). At the same time, mineralized bone formation had just begun in the Runx2^{het} embryos but it was completely absent in the Double^{het} embryos (Fig. 3). At 17.5 and 18.5 dpc, WT and Osx^{het} embryos continued to exhibit normal bone formation, while Runx2^{het} and Double^{het} embryos showed delayed bone formation (Fig. 3 and data not shown). Especially, the region of hypertrophic chondrocytes was expanded and the area of mineralized bones was clearly reduced in the humerus of the Double^{het} embryos. The region of ColX expression, which was examined in the hypertrophic zone of the growth plates, was remarkably expanded in the Double^{het} embryos (data not shown), indicating that chondrocyte differentiation was delayed. These results indicate that bone formation is remarkably delayed in Double^{het} embryos compared to the other genotypes.

3.3. Expression profile of genes regulated in Double^{het} embryos during skeletal development

To elucidate the correlation between Runx2 and Osx, microarray analysis was performed at 17.5 dpc in WT, Runx2^{het}, Osx^{het}, and Double^{het} embryos. A total of 7703 genes had differential

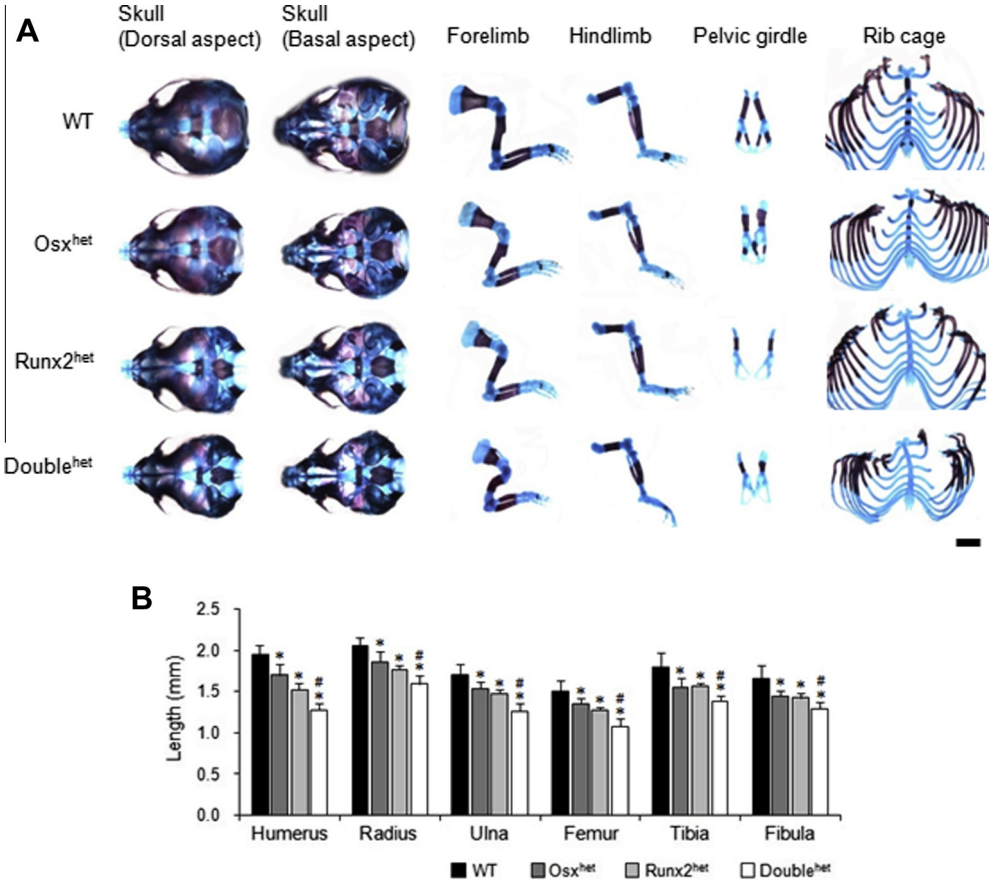

Fig. 2. Analysis of the skeletal phenotypes of Double^{het} embryos. (A) Higher magnification of each bone in Fig. 1B. Skull defects, small rib cage, and short limbs were observed in the Double^{het} embryos. The ribs and humerus were bent. No difference was observed between the WT and Osx^{het} embryos. Scale bar = 1 mm. (B) The length of all long bones in the forelimb and hindlimb was significantly reduced in the Double^{het} embryos. $^{*}p < 0.05$.

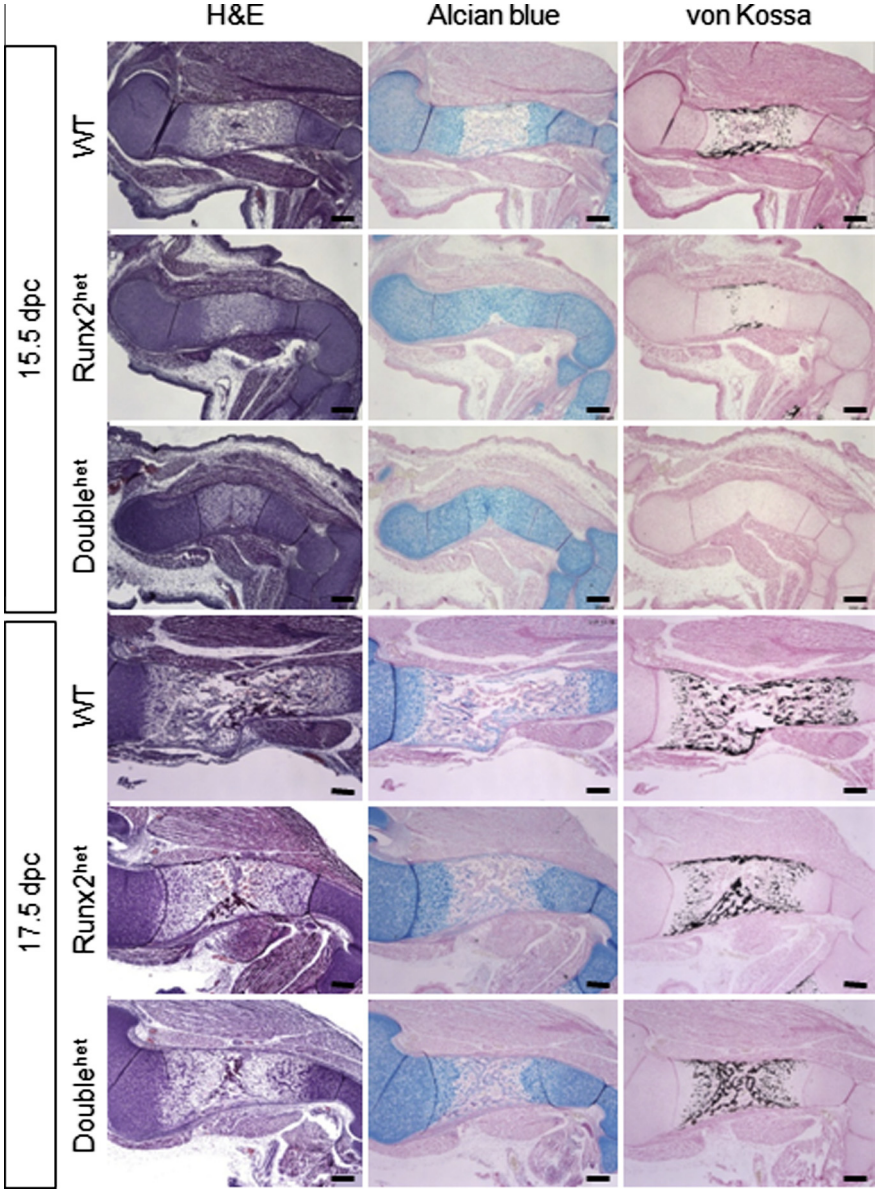

Fig. 3. Histological analysis of the Double^{het} embryos. Histological analysis using H&E, alcian blue, and von Kossa staining was performed in the humerus at 15.5 and 17.5 dpc. During skeletal development, the region of hypertrophic chondrocytes was expanded and the area of mineralized bones was reduced in the Double^{het} embryos. Scale bar = 200 μm. (For interpretation of the references to color in this figure legend, the reader is referred to the web version of this article.)

expression in the embryos. Gene clustering was performed for genes with similar expression patterns with at least a twofold change. Cluster 1 includes 68 genes that were the most downregulated in the Double^{het} embryos (Fig. 4A). This cluster contains 22 genes that were identified by gene ID or symbol, including chondrogenesis-related genes such as type II collagen alpha 1 (*Col2a1*), SRY-box containing gene 9 (*Sox9*), and aggrecan (*Acan*) (Table 1). Cluster 2 includes 18 upregulated genes in the Double^{het} embryos (Fig. 4B). Seventeen genes were identified by gene ID or symbol, for example, dermatopontin (*Dpt*), osteocrin (*Ostn*), and calsequestrin 1 (*Casq1*) (Table 1). This analysis suggests that skeletal development may be controlled by multiple genes that are regulated by both Runx2 and Osx.

4. Discussion

Bone formation is regulated by various genes and their signaling pathway. Especially, the BMP signaling pathway and major key transcription factors Runx2 and Osx are the most important for bone formation. Many studies have reported an altered phenotype and function due to the lack of each gene involved in bone development. In this study, we investigated the skeletal phenotype and differential gene expression resulting from the lack of both Runx2 and Osx.

Double^{het} embryos were generated by intercrossing Runx2$^{\Delta C/+}$ and Osx$^{+/-}$ heterozygous mice [7,10], but it was difficult to obtain viable Double^{het} neonates. Skeletal analysis of Double^{het} embryos showed the formation of a hypoplastic thoracic cage, followed by possible respiratory failure. Thus, Double^{het} embryos are expected to survive until parturition but die after birth. A previous study reported that Runx2^{het} embryos have normal skeletons and craniofacial features, but they lack clavicles [7]. Nevertheless, a detailed skeletal analysis of the Runx2^{het} embryos was performed in this study. Although the skeletons from the Runx2^{het} embryos showed weaker defects than the Double^{het} embryos, the former showed skull defects, lack of clavicles, pelvic girdle, and deltoid tuberosity,

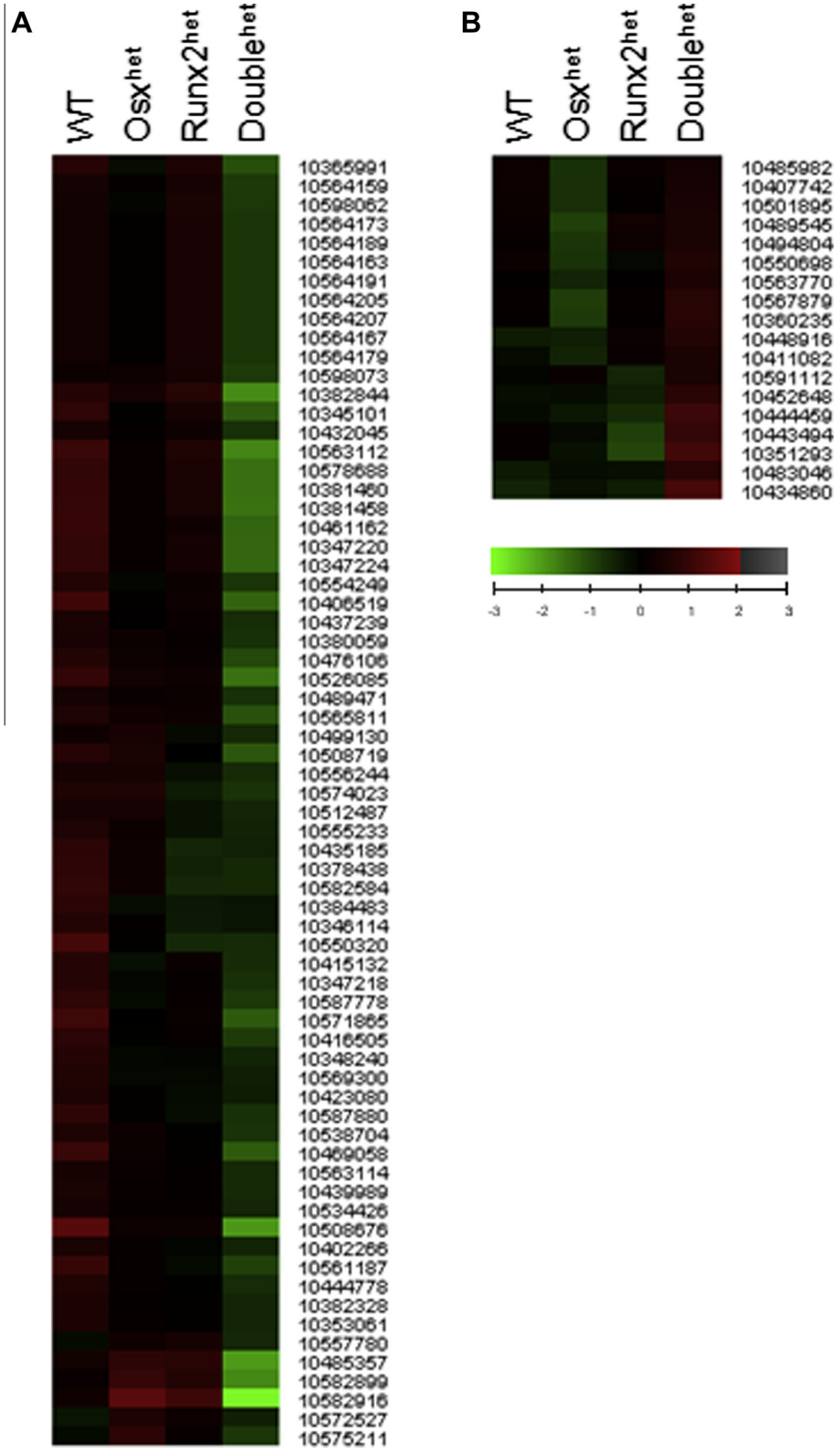

Fig. 4. Classification of differentially expressed genes with a similar expression pattern in the embryos. (A) Cluster 1 includes genes that are downregulated in the Double^{het} embryos. (B) Cluster 2 includes genes that are upregulated in the Double^{het} embryos. All data from the microarray were filtered to identify genes that exhibit a twofold or greater difference in expression between the groups. Each number in the column on the right indicates the probe ID.

and a short skeleton. This result indicates that haploinsufficiency of the function of the Runx2 C-terminus during embryonic development prevents the formation of many other bones in addition to clavicles. Moreover, skeletons of the Double^{het} embryos exhibited significant and additive differences in the endochondral and intramembranous bone formation. Compared to the other embryos, Double^{het} embryos showed a significant reduction in the bone length of their limbs. Severe bending and delayed bone formation

Table 1
Differentially expressed genes in response to Runx2/Osx double heterozygote (Double^{het}) embryos.

Probe ID	Gene assignment	Gene title (symbol)
Downregulated genes in response to Double^{het}		
10365991	NM_007884	Epiphycan (Epyc)
10345101	NM_007740	Collagen, type IX, alpha 1 (Col9a1)
10432045	BC082331	Collagen, type II, alpha 1 (Col2a1)
10461162	NR_002896	Small nucleolar RNA host gene (non-protein coding) 1 (Snhg1)
10554249	NM_007424	Aggrecan (Acan)
10406519	ENSMUST00000022108	Hyaluronan and proteoglycan link protein 1 (Hapln1)
10489471	ENSMUST00000103104	Matrilin 4 (Matn4)
10565811	NR_002173	RNA, U15b small nucleolar (Rnu15-b)
10556244	AK039338	Importin 7 (Ipo7)
10574023	NM_008630	Metallothionein 2 (Mt2)
10512487	NR_001460	RNA component of mitochondrial RNAase P (Rmrp)
10415132	NM_026066	CKLF-like MARVEL transmembrane domain containing 5 (Cmtm5)
10571865	NM_009136	Scrapie responsive gene 1 (Scrg1)
10416505	NM_026214	Potassium channel tetramerization domain containing 4 (Kctd4)
10569300	NM_001037822	Keratin associated protein 5–5 (Krtap5–5)
10423080	NM_030888	C1q and tumor necrosis factor related protein 3 (C1qtnf3)
10587880	NM_029620	Procollagen C-endopeptidase enhancer 2 (Pcolce2)
10469058	EF529510	RIKEN cDNA 1110017I16 gene
10508676	ENSMUST00000102576	Matrilin 1, cartilage matrix protein 1 (Matn1)
10561187	BC009815	Melanoma inhibitory activity 1 (Mia1)
10382328	ENSMUST00000000579	SRY-box containing gene 9 (Sox9)
10575211	BC021524	WW domain containing E3 ubiquitin protein ligase 2 (Wwp2)
Upregulated genes in response to Double^{het}		
10485982	NM_009608	Actin, alpha, cardiac (Actc1)
10407742	NM_033268	Actinin alpha 2 (Actn2)
10501895	ENSMUST00000029761	Myozenin 2 (Myoz2)
10489545	NM_009394	Troponin C2, fast (Tnnc2)
10494804	NM_009814	Calsequestrin 2 (Casq2)
10550698	NM_007710	Creatine kinase, muscle (Ckm)
10563770	NM_013808	Cysteine and glycine-rich protein 3 (Csrp3)
10567879	NM_007504	ATPase, Ca^{2+} transporting, cardiac muscle, fast twitch
10360235	NM_009813	1(Atp2a1)
10411082	ENSMUST00000022213	Calsequestrin 1 (Casq1)
10591112	NM_001080814	Thrombospondin 4 (Thbs4)
10452648	NM_145158	FAT tumor suppressor homolog 3 (Drosophila) (Fat3)
10444459	NM_031176	Elastin microfibril interfacer 2 (emilin2)
10443494	AB046537	Tenascin XB (Tnxb)
10351293	NM_019759	Peptidase inhibitor 16 (Pi16)
10483046	ENSMUST00000047812	Dermatopontin (Dpt)
10434860	NM_198112	Dipeptidylpeptidase 4 (Dpp4)
		Osteocrin (Ostn)

were prominently observed in the humerus of the Double^{het} embryos, suggesting that both Runx2 and Osx are more important for the bone formation of the humerus than the other bones. In histological analysis, mineralization was observed in WT embryos; however, no difference in phenotype between the Double^{het} embryos and the other embryos was detected at 14.5 dpc. After 15.5 dpc, compared to normal mineralization in WT and Osx^{het} embryos, delayed mineralization was observed in Runx2^{het} embryos and no mineralization was exhibited in Double^{het} embryos. Delayed bone formation was also confirmed by *LacZ* gene expression elucidated with X-gal staining. The Osx heterozygous mice have the *LacZ* gene knocked-into the *Osx* locus to recapitulate the Osx expression in the bone by X-gal staining [10]. Thus, the altered bone formation can be represented by X-gal staining between Osx^{het} and Double^{het} embryos at 17.5 dpc (unpublished data). Overall, the Double^{het} embryos showed diminished LacZ expression. The interparietal bone was missing and the ribs were bent. Weak and irregular LacZ expression was observed in the Double^{het} embryos compared to the Osx^{het} embryos. Therefore, regulation by both Runx2 and Osx may be essential for skeletal development.

DNA microarray analysis was performed to obtain information about the differentially expressed genes in WT, Osx^{het}, Runx2^{het}, and Double^{het} embryos at 17.5 dpc. Microarray data were classified according to similarities in gene expression patterns. For the classification of cluster 1, the gene expression was progressively downregulated in the following order: WT, Runx2^{het}, Osx^{het}, and Double^{het}, or WT, Osx^{het}, Runx2^{het}, and Double^{het}. Epiphycan (*Epyc*), *Col9a1*, *Col2a1*, and *Sox9* are genes that are involved in bone formation that were included in cluster 1. Several genes including *C1q*, tumor necrosis factor-related protein 3 (*C1qtnf3*), and WW domain-containing E3 ubiquitin protein ligase 2 (*Wwp2*) also showed the same expression pattern as *Sox9* and *Col9a1*. Among them, *Epyc* is a member of the small leucine-rich proteoglycan family that was isolated from epiphyseal cartilage that plays a role in bone formation and cartilage matrix organization [15,16]. It has been reported that C1qtnf3 regulates embryonic cartilage development and postnatal bone growth, and it promotes vascular calcification and osteosarcoma cell proliferation [17,18]. While the ubiquitin E3 ligase Wwp1 negatively regulates osteoblast function by inhibiting osteoblast differentiation and migration [19], Wwp2 controls craniofacial patterning by interacting with a paired-like homeobox transcription factor, goosecoid, which is important in craniofacial development [20]. In contrast, cluster 2 includes genes that are upregulated in the Double^{het} embryos compared to the other groups. Genes including *Dpt*, *Ostn*, and *Casq1* were highly increased in the Double^{het} embryos. A downstream target of the vitamin D receptor Dpt inhibits BMP-stimulated alkaline phosphatase activity in osteoblast differentiation [21,22]. Ostn, a bone-active molecule, is highly expressed in osteoblastic lineage cells and is a vitamin D-regulated protein that modulates the osteoblast phenotype [23,24]. It has a role in the natriuretic peptide clearance

of the skeleton, finally modulating bone growth [25]. However, although these genes were remarkably upregulated or downregulated in the Double^{het} embryos, Runx2-related or Osx-related functions are not well studied. Further studies will be required to determine the molecular mechanisms of these genes regulated by Runx2 and Osx in bone formation. To the best of our knowledge, this is the first study to establish the correlation between Runx2 and Osx. In the future, this study may facilitate the understanding of the mechanism of the *Runx2* and *Osx* genes in skeletal development and bone diseases.

Conflicts of interest

The authors state that they have no conflicts of interest.

Acknowledgment

This study was supported by the Korea Research Foundation Grant funded by the Korea Government (KRF-2008-331-E00039).

References

[1] T. Mishina, M.W. Starbuck, M.A. Gentile, T. Fukuda, V. Kasparcova, J.G. Seedor, M.C. Hanks, M. Amling, G.J. Pinero, S. Harada, R.R. Behringer, Bone morphogenetic protein type IA receptor signaling regulates postnatal osteoblast function and bone remodeling, J. Biol. Chem. 279 (2004) 27560–27566.
[2] R.D. Devlin, Z. Du, R.C. Pereira, R.B. Kimble, A.N. Economides, V. Jorgetti, E. Canalis, Skeletal overexpression of noggin results in osteopenia and reduced bone formation, Endocrinology 144 (2003) 1972–1978.
[3] X.B. Wu, Y. Li, A. Schneider, W. Yu, G. Rajendren, J. Iqbal, M. Yamamoto, M. Alam, L.J. Brunet, H.C. Blair, M. Zaidi, E. Abe, Impaired osteoblastic differentiation, reduced bone formation, and severe osteoporosis in noggin-overexpressing mice, J. Clin. Invest. 112 (2003) 924–934.
[4] Y. Yoshida, S. Tanaka, H. Umemori, O. Minowa, M. Usui, N. Ikematsu, E. Hosoda, T. Imamura, J. Kuno, T. Yamashita, K. Miyazono, M. Noda, T. Noda, T. Yamamoto, Negative regulation of BMP/Smad signaling by Tob in osteoblasts, Cell 103 (2000) 1085–1097.
[5] J. Hanai, L.E. Chen, T. Kanno, N. Ohtani-Fujita, W.Y. Kim, W.H. Guo, T. Imamura, Y. Ishidou, M. Fukuchi, M.J. Shi, J. Stavnezer, M. Kawabata, K. Miyazono, Y. Ito, Interaction and functional cooperation of PEBP2/CBF with Smads. Synergistic induction of the immunoglobulin germline C alpha promoter, J. Biol. Chem. 274 (1999) 31577–31582.
[6] R. Nishimura, K. Hata, S.E. Harris, F. Ikeda, T. Yoneda, Core-binding factor alpha 1 (Cbfa1) induces osteoblastic differentiation of C2C12 cells without interactions with Smad1 and Smad5, Bone 31 (2002) 303–312.
[7] J.Y. Choi, J. Pratap, A. Javed, S.K. Zaidi, L. Xing, E. Balint, S. Dalamangas, B. Boyce, A.J. van Wijnen, J.B. Lian, J.L. Stein, S.N. Jones, G.S. Stein, Subnuclear targeting of Runx2/Cbfa/AML factors is essential for tissue-specific differentiation during embryonic development, Proc. Natl. Acad. Sci. U.S.A. 98 (2001) 8650–8655.
[8] T. Komori, H. Yagi, S. Nomura, A. Yamaguchi, K. Sasaki, K. Deguchi, Y. Shimizu, R.T. Bronson, Y.H. Gao, M. Inada, M. Sato, R. Okamoto, Y. Kitamura, S. Yoshiki, T. Kishimoto, Targeted disruption of Cbfa1 results in a complete lack of bone formation owing to maturational arrest of osteoblasts, Cell 89 (1997) 755–764.
[9] F. Otto, A.P. Thornell, T. Crompton, A. Denzel, K.C. Gilmour, I.R. Rosewell, G.W. Stamp, R.S. Beddington, S. Mundlos, B.R. Olsen, P.B. Selby, M.J. Owen, Cbfa1, a candidate gene for cleidocranial dysplasia syndrome, is essential for osteoblast differentiation and bone development, Cell 89 (1997) 765–771.
[10] K. Nakashima, X. Zhou, G. Kunkel, Z. Zhang, J. Deng, M. Owen, R. Behringer, B. de Crombrugghe, The novel zinc finger-containing transcription factor osterix is required for osteoblast differentiation and bone formation, Cell 108 (2002) 17–29.
[11] M. Phimphilai, Z. Zhao, H. Boules, H. Roca, R.T. Franceschi, BMP signaling is required for RUNX2-dependent induction of the osteoblast phenotype, J. Bone Miner. Res. 21 (2006) 637–646.
[12] M.H. Lee, Y.J. Kim, H.J. Kim, H.D. Park, A.R. Kang, H.M. Kyung, J.H. Sung, J.M. Wozney, H.J. Kim, H.M. Ryoo, BMP-2-induced Runx2 expression is mediated by Dlx5, and TGF-beta 1 opposes the BMP-2-induced osteoblast differentiation by suppression of Dlx5 expression, J. Biol. Chem. 278 (2003) 34387–34394.
[13] M.H. Lee, T.G. Kwon, H.S. Park, J.M. Wozney, H.M. Ryoo, BMP-2-induced Osterix expression is mediated by Dlx5 but is independent of Runx2, Biochem. Biophys. Res. Commun. 309 (2003) 689–694.
[14] T. Matsubara, K. Kida, A. Yamaguchi, K. Hata, F. Ichida, H. Meguro, H. Aburatani, R. Nishimura, T. Yoneda, BMP2 regulates Osterix through Msx2 and Runx2 during osteoblast differentiation, J. Biol. Chem. 283 (2008) 29119–29125.
[15] H.J. Joohnson, L. Rosenberg, H.U. Choi, S. Garza, M. Höök, P.J. Neame, Characterization of epiphycan, a small proteoglycan with a leucine-rich repeat core protein, J. Biol. Chem. 272 (1997) 18709–18717.
[16] S. Nuka, W. Zhou, S.P. Henry, C.M. Gendron, J.B. Schultz, T. Shinomura, J. Johnson, Y. Wang, D.R. Keene, R. Ramírez-Solis, R.R. Behringer, M.F. Young, M. Höök, Phenotypic characterization of epiphycan-deficient and epiphycan/biglycan double-deficient mice, Osteoarthr. Cartil. 18 (2010) 88–96.
[17] H. Akiyama, S. Furukawa, S. Wakisaka, T. Maeda, Elevated expression of CTRP3/cartducin contributes to promotion of osteosarcoma cell proliferation, Oncol. Rep. 21 (2009) 1477–1481.
[18] Y. Zhou, J.Y. Wang, H. Feng, C. Wang, L. Li, D. Wu, H. Lei, H. Li, L.L. Wu, Overexpression of c1q/tumor necrosis factor-related protein-3 promotes phosphate-induced vascular smooth muscle cell calcification both in vivo and in vitro, Arterioscler. Thromb. Vasc. Biol. 34 (2014) 1002–1010.
[19] L. Shu, H. Zhang, B.F. Boyce, L. Xing, Ubiquitin E3 ligase Wwp1 negatively regulates osteoblast function by inhibiting osteoblast differentiation and migration, J. Bone Miner. Res. 28 (2013) 1925–1935.
[20] W. Zou, X. Chen, J.H. Shim, Z. Huang, N. Brady, D. Hu, R. Drapp, K. Sigrist, L.H. Glimcher, D. Jones, The E3 ubiquitin ligase Wwp2 regulates craniofacial development through mono-ubiquitylation of goosecoid, Nat. Cell Biol. 13 (2011) 59–65.
[21] R.R. Pochampally, J. Ylostalo, P. Penfornis, R.R. Matz, J.R. Smith, D.J. Prockop, Histamine receptor H1 and dermatopontin: new downstream targets of the vitamin D receptor, J. Bone Miner. Res. 22 (2007) 1338–1349.
[22] K. Behnam, S.S. Murray, E.J. Brochmann, BMP stimulation of alkaline phosphatase activity in pluripotent mouse C2C12 cells is inhibited by dermatopontin, one of the most abundant low molecular weight proteins in demineralized bone matrix, Connect. Tissue Res. 47 (2006) 271–277.
[23] S. Bord, D.C. Ireland, P. Moffatt, G.P. Thomas, J.E. Compston, Characterization of osteocrin expression in human bone, J. Histochem. Cytochem. 53 (2005) 1181–1187.
[24] G. Thomas, P. Moffatt, P. Salois, M.H. Gaumond, R. Gingras, E. Godin, D. Miao, D. Goltzman, C. Lanctôt, Osteocrin, a novel bone-specific secreted protein that modulates the osteoblast phenotype, J. Biol. Chem. 278 (2003) 50563–50571.
[25] P. Moffatt, G. Thomas, K. Sellin, M.C. Bessette, F. Lafrenière, O. Akhouayri, R. St-Arnaud, C. Lanctôt, Osteocrin is a specific ligand of the natriuretic peptide clearance receptor that modulates bone growth, J. Biol. Chem. 282 (2007) 36454–36462.